Acta Geotechnica (2022) 17:4921–4933
https://doi.org/10.1007/s11440-022-01672-9

RESEARCH PAPER

Effect of fines content on soil freezing characteristic curve of sandy soils

Quoc Hung Vu[1] · Jean-Michel Pereira[1] · Anh Minh Tang[1]

Received: 17 December 2021 / Accepted: 1 August 2022 / Published online: 3 October 2022

Abstract
Soil freezing characteristic curve (SFCC) represents the relationship between soil temperature and unfrozen water content of soil during freezing and thawing processes. In this study, SFCC of sandy soils was determined in laboratory. Pure sand was mixed with clay at various contents (0, 5, 10, 15, and 20% of the total dry mass), and the mixtures were compacted to their respective maximum dry density. Compacted specimens were then placed in a close and rigid cell, and the soil's temperature was decreased step-by-step to freeze the soil water and then increased back to thaw it. During this thermal cycle, soil's temperature and volumetric water content were monitored in order to determine the SFCC. The results show that SFCC was strongly dependent on the fines content: at higher fines content, the temperature of spontaneous nucleation was lower, and the residual unfrozen volumetric water content was higher.

Keywords Hysteresis · Residual water content · Soil freezing characteristic curve · Temperature of spontaneous nucleation

1 Introduction

Frozen soil consists of mineral particles, liquid water, ice and gas. It is formed from unfrozen soil during freezing, when a fraction of liquid water solidifies into ice at temperatures sufficiently low below 0 °C [2]. This phase change causes significant modifications of physical–hydraulic–mechanical properties of soils [3]. The freezing–thawing process is encountered in cold regions, seasonal cold regions as well as construction works using artificial ground freezing technique. Two main consequences of this process that need to be mentioned are frost heave and thaw settlement. These phenomena can induce damages to infrastructure [26, 56, 86, 87].

The freezing–thawing process in porous media has been investigated not only in civil engineering and geosciences but also in physics [1, 19, 39, 41, 49]. While bulk water melts at 0 °C, water in porous media melts at temperatures below 0 °C because of physical interactions between water and solid particles [22, 53, 58]. Freezing process of a soil sample (where heat is extracted from the sample with a constant rate) can be divided into three steps (as shown in Fig. 1): (i) supercooling with release of sensible heat; (ii) first water freezing with release of latent heat; (iii) further water freezing with release of sensible heat. In the first step, during cooling (extraction of heat from soil), soil temperature decreases to reach a certain value from that it cannot decrease anymore. This value is called temperature of spontaneous nucleation T_{sn} where the first ice embryo nucleus forms because it attains the critical size [4, 5]. Formation of ice crystals releases latent heat and thus increases soil temperature. From T_{sn}, soil temperature increases to reach another value which is called freezing temperature T_f, where it remains on a plateau for a while. During this second step, soil water is gradually frozen along with releasing latent heat. After that, within the third step, soil temperature decreases with further water freezing. Freezing temperature T_f, also considered to be equal to thawing temperature T_t at which soil state changes from frozen to unfrozen, is usually used as a boundary value index to distinguish between frozen soil and unfrozen soil [74, 85, 90]. These characteristic temperatures (T_{sn} and T_f) were investigated in several studies [4, 11, 90].

✉ Anh Minh Tang
anh-minh.tang@enpc.fr

[1] Laboratoire Navier, Ecole des Ponts ParisTech, Univ Gustave Eiffel, CNRS, 6-8 Avenue Blaise Pascal, 77455 Marne-la-Vallée, France

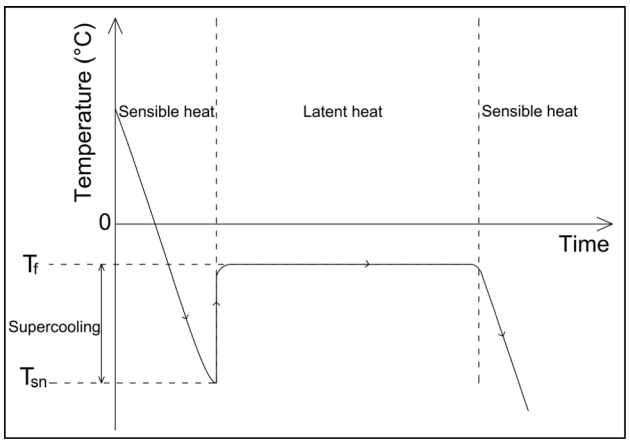

Fig. 1 Freezing process of soil–water system

Soil freezing characteristic curve (SFCC) represents the relationship between the temperature and the quantity of liquid water in soil. It is one of the most essential data in studying the freezing–thawing process in soils. On the one hand, several SFCC models were empirically developed. From SFCC obtained experimentally, empirical models were proposed using power, piecewise or exponential functions [9, 24, 29, 40, 43, 67, 69, 81]. On the other hand, SFCC can be derived from soil water characteristic curve (SWCC). This approach is based on the theory of similarity between freezing–thawing and drying–wetting processes that is illustrated by Clapeyron equation [20, 35, 46, 59, 64, 66, 88, 89, 95]. More generally, various physical models were developed based on theory of capillarity, sorption or that of interface pre-melting [33, 76, 92]. Most of the existing SFCC models consider the effect of fines content, but this effect is considered in different ways. For instance, some empirical models used specific surface or liquid limit as input data, while physics-based models consider absorption parameters of soil. Due to the diversity of SFCC models, there is no unified standard for choosing SFCC in numerical simulations [12]. In addition, except few models (e.g. [95]), most of the existing ones consider a unique relationship between unfrozen water content and temperature. However, this relation obtained on the freezing path can differ from that of the thawing path; at a given temperature, water content of the freezing path can be higher than at of the thawing path. This hysteresis is usually ignored in the models.

To determine SFCC in the laboratory, a soil specimen is usually subjected to a freeze–thaw cycle, while unfrozen water content is measured. Although controlling specimen's temperature is technically feasible, measuring unfrozen water content is much more challenging. Several methods and techniques have been developed to evaluate the unfrozen water content at negative temperature, including dilatometry [37, 52], gas dilatometry [61], adiabatic calorimetry [8, 36], isothermal calorimetry [69], differential scanning calorimetry [38, 39, 83], X-ray diffraction [6, 7], time/frequency domain reflectometry (TDR/FDR) [57, 63, 94] and pulsed nuclear magnetic resonance (P-NMR) [45, 70, 76]. Among these methods, TDR and P-NMR are the two most common ones. P-NMR is widely acknowledged as a highly accurate and non-destructive technique. However, the equipment required for this technique is generally expensive [84]. Compared to P-NMR, TDR/FDR can be used in the laboratory as well as in the field, and it is cheaper, quicker, and more portable. With TDR, unfrozen water content is inferred from the measurement of apparent dielectric constant of soil using an empirical equation [60, 71] or dielectric mixing models [55, 63, 77]. It is noted that several factors such as temperature or bound water can affect its accuracy.

Several studies have determined SFCC in the laboratory in both freezing and thawing processes [16, 31, 33, 37, 45, 62, 68, 90]. These studies recognized that hysteresis exists in SFCC in which the unfrozen water content is different in thawing and freezing processes at the same temperature. Hysteresis in freezing–thawing process was believed to be similar to that of wetting–drying process. However, the mechanism inducing hysteresis in SFCC is complex and it may be influenced by several effects such as supercooling, pore blocking, capillarity, free energy barriers, contact angles and electrolytes [16, 45]. It is also noted that hysteresis is significant at temperatures between -2 and 0 °C [32, 37, 44] and that it should not be ignored due to impacts on unfrozen water content on frost heaving [30, 72], creep behaviour of frozen soils [10, 91] as well as thermal regime of frozen ground [21].

Beside hysteresis effect, it is found that the shape of SFCC depends also on several factors, including liquid limit [69], stress condition [50], salt content and solute types [48, 76], initial water content or degree of saturation [34, 65, 80], types of soil [16, 44, 90], pore-size distribution [45], and fines content [45, 68, 69, 90]. Among these factors, fines content can influence others (liquid limit, pore-size distribution and types of soil). As far as fines content is concerned, by determining unfrozen water content of several clays, a silt and a gravel, Tice et al. [69] observed significantly different unfrozen water contents at the same temperature below 0 °C. Tian et al. [68] carried out tests on three soils corresponding to three clay contents and found that unfrozen water degree of saturation also changed in different ways in both freezing and thawing processes. For soils containing higher clay fraction, unfrozen water degree of saturation was higher at any given temperature below freezing point and the hysteresis loop was smaller. The same findings concerning SFCC were obtained in the study of Zhang et al. [90] on silty clay, and silt and in the study of Li et al. [45] on silty clay, fine

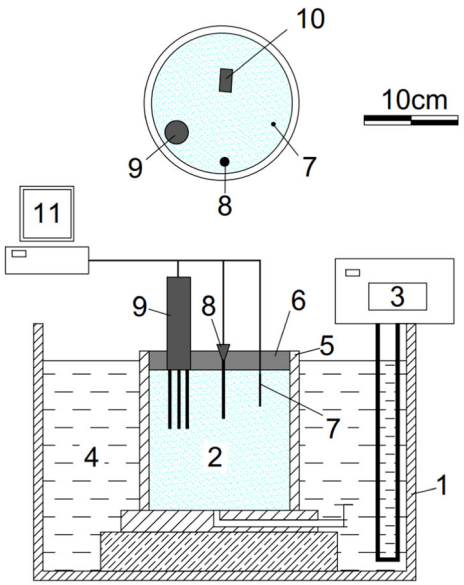

Fig. 2 Schematic view of the experimental setup. (1) Temperature-controlled bath; (2) soil specimen; (3) temperature controlling system; (4) temperature-controlled liquid (30% ethylene glycol + 70% water); (5) metallic cylindrical cell; (6) insulating cover; (7) temperature sensor; (8) tensiometer; (9) soil water sensor; (10) thermal conductivity probe (results are not presented in this study); (11) data logger system

sand, and medium sand. Some other authors also investigated different soils, but the effect of fines content was out of their focus [16, 66, 67, 70].

The present study aims at systematically investigating the effect of fines content on the SFCC of sandy soils. Clean sand was mixed with clay at dry state firstly and water afterwards to obtain sandy soils with clay content of 0, 5, 10, 15, and 20% prior to compaction at the Proctor maximum dry density followed by a saturation phase. The specimen's temperature was then decreased progressively to freeze the soil specimen in undrained conditions prior to applying the thawing process. During this freezing–thawing cycle, soil's temperature and unfrozen water content were measured. After the introduction, the second section of this paper presents the materials and experimental methods. Experimental results are presented in the third section, before being discussed in the fourth section.

2 Materials and experimental methods

2.1 Experimental setup

The experimental setup is shown in Fig. 2, and the details of the sensors used are presented in Table 1. Soil specimen was contained in a rigid metallic cylindrical cell (150 mm in height and 150 mm in diameter). The cell was immerged in a temperature-controlled bath (F38-EH JULABO with ± 0.03 °C accuracy). Soil temperature was measured with a PT100 sensor, soil volumetric water content was measured with a ML2x Thetaprobe sensor, and soil suction was measured with a tensiometer. As Thetaprobe sensor measures soil apparent dielectric constant (K_a) which is the ratio of the dielectric permittivity of a substance to free space, soil unfrozen volumetric water content (θ_u) was estimated from measured K_a by using empirical equations of Smith and Tice [60] (1) and Topp et al. [71] (2) for frozen and unfrozen states of soil, respectively. Equation (2) is used only for the initial state (before the occurrence of freezing) and for the final state where thawing is complete. Equation (1) is used where ice is expected to exist in soil (i.e. after the occurrence of freezing and before the completion of thawing).

$$\theta_u = -0.1458 + 3.868 \times 10^{-2} \times K_a - 8.502 \times 10^{-4} \times K_a^2 + 9.92 \times 10^{-6} \times K_a^3 \quad (1)$$

$$\theta_u = -5.3 \times 10^{-2} + 2.92 \times 10^{-2} \times K_a - 5.5 \times 10^{-4} \times K_a^2 + 4.3 \times 10^{-6} \times K_a^3 \quad (2)$$

2.2 Material

Fontainebleau sand was carefully mixed with Speswhite kaolin clay at dry state using an automatic mortar mixer in order to obtain sandy soils with fines content (dry mass of clay divided by dry mass of soil) of 0, 5, 10, 15, and 20%. The physical properties of sand and clay are shown in Tables 2 and 3, respectively. Figure 3 presents the grain

Table 1 Properties of sensors using in freezing–thawing tests

Measured parameters	Principle	Type	Accuracy	Range
Temperature	Resistance temperature detector	PT100	± 0.03 °C	−200 to 400 °C
Volumetric unfrozen water content	Time domain reflectometry (dielectric constant)	ThetaProbe ML2x (4 rods)	0.01 m^3/m^3	0.01 to 1 m^3/m^3
Tensiometer	Piezoelectric transducer	T5x	± 0.5 kPa	−160 to 100 kPa
Thermal conductivity	Transient line heat source	KD2-Prob (RK-1)	10%	0.1 to 4 W/(m K)

Table 2 Physical properties of sand

Property	Value
Median grain size, D_{50} (mm)	0.21
Uniformity coefficient, C_U	1.52
Minimum void ratio, e_{min}	0.54
Maximum void ratio, e_{max}	0.94
Particle density, ρ_s (Mg/m^3)	2.65
Minimum dry density, $\rho_{d,min}$ (Mg/m^3)	1.37
Maximum dry density, $\rho_{d,max}$ (Mg/m^3)	1.72

Table 3 Physical properties of clay

Property	Value
Liquid limit, LL (%)	55
Plastic limit, PL (%)	30
Plasticity index, PI	25
Specific surface area (m^2/g)	0.94
Particle density, ρ_s (Mg/m^3)	2.65
Particle diameter < 0.002 mm (%)	79
Particle diameter > 0.01 mm (%)	0.5
Maximum dry density, $\rho_{d,max}$ (Mg/m^3)	1.45

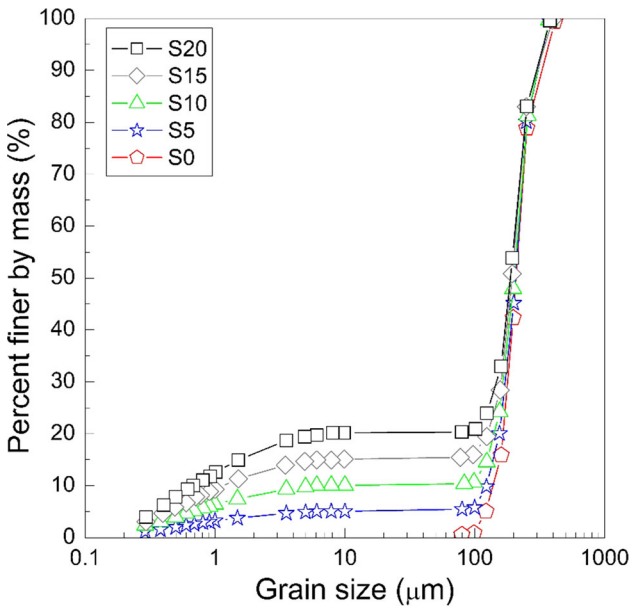

Fig. 3 Grain size distribution curves

size distribution of these soils. In this study, the name of each soil corresponds to its clay content (for instance, S10 corresponds to a soil having 10% of clay in dry mass). Prior to the preparation of the soil specimens, each soil was carefully mixed with distilled water using the mortar mixer to obtain optimum water content (determined from the Normal Proctor compaction curves obtained on the same soils [17]). Afterwards, wet soil was packed in a plastic bag for at least 24 h to ensure the homogenisation of water content, prior to compaction in the cylindrical cell to reach its maximum dry density.

2.3 Experimental procedure

After soil compaction in the cell, sensors were installed as shown in Fig. 2 and an insulating cover made of expanded polystyrene was placed in order to avoid heat exchange between soil specimen and ambient air. The whole system was then transferred inside the temperature-controlled bath. Prior to the freezing–thawing test, soil specimen was saturated by injecting water from the bottom of the specimen during 0.5–2 days depending on fines content. After the saturation (when a layer of water of 10 mm was visible on the top of the specimen), the temperature of the bath was first set at a temperature between 0 and −1 °C (slightly higher than the expected T_{sn}). Each test started with the cooling path. The bath temperature was decreased in steps of 0.1 °C to freeze the soil pore water. Once the freezing was triggered, the temperature continued to be decreased in steps of 0.2 °C until −2 or −3 °C to observe the change of liquid water content during further cooling. Afterwards, during the heating path, the bath temperature was increased in steps of 0.2 °C until 0 °C to thaw the frozen soil. During both cooling and heating paths, the bath temperature was changed to the subsequent step only when soil temperature and volumetric unfrozen water content (measured by the sensors) had reached their equilibrium state. The equilibrium state was considered reached when these two quantities did not change (< 0.05 °C for temperature and < 1% for water content) during at least 2 h.

The test programme is shown in Table 4. The test number shows the soil tested (S0 to S20) followed by the number of replicate test (T1 to T4). At least two tests were performed for each soil. Tests T1 were performed following the procedure described above to obtain the complete SFCC curves. For the other tests (T2, T3, T4), only the freezing path of the same procedure was performed in order to replicate the characteristic temperatures.

3 Experimental results

3.1 Typical test (S10-T1)

As an example, the results of test S10-T1 are shown in Fig. 4 where soil temperature, suction, and volumetric unfrozen water content are plotted versus elapsed time for the cooling path.

Table 4 Physical properties of soils

Test no	Fines content (%)	Dry density (Mg/m^3)	Porosity (–)	Test duration (h)
S20-T1	20	1.98	0.25	754
S20-T2	20	1.96	0.26	26
S15-T1	15	1.99	0.25	712
S15-T2	15	2.00	0.25	64
S10-T1	10	1.91	0.28	590
S10-T2	10	1.90	0.28	153
S5-T1	5	1.78	0.33	817
S5-T2	5	1.78	0.33	143
S5-T3	5	1.78	0.33	190
S0-T1	0	1.67	0.37	756
S0-T2	0	1.67	0.37	286
S0-T3	0	1.67	0.37	75
S0-T4	0	1.68	0.37	187

From −1.2 °C, soil temperature was decreased in steps of 0.1 °C down to −1.6 °C. During this period, soil temperature was controlled through the bath's temperature, suction remained equal to zero and volumetric water content remained constant. When soil temperature reached −1.6 °C, soil freezing started inducing abrupt changes in the three measured quantities. Results obtained during this stage (elapsed time of 70–86 h) are shown in Fig. 5 for a better view.

As shown in Fig. 5, when the bath temperature was changed from −1.5 to −1.6 °C (at 76 h), soil temperature changed to −1.6 °C after a few minutes. At 77 h, while the bath temperature was still maintained at −1.6 °C, soil temperature increased abruptly to −0.1 °C prior to a progressive decrease and reached the imposed temperature (−1.6 °C) again at 83 h. Soil suction started to increase at 78 h and reached a maximum value of 300 kPa prior to fall down to 100 kPa. At 77 h, soil water content decreased abruptly from 28 to 26% prior to decrease progressively to 3% at 82 h. These results are representative of a freezing process in soil (Fig. 1) where the phase before 77 h corresponds to the supercooling step. At 77 h, soil water started to freeze: soil temperature increased abruptly because of latent heat release prior to decrease because of heat diffusion towards the liquid surrounding the cell; soil suction increased quickly because of the cryogenic suction induced by ice formation in the pore space (the sudden decrease in suction from 300 to 100 kPa corresponded to the cavitation of the tensiometer, after this moment, the sensor did not provide anymore the real soil suction); volumetric water content decreased because of ice formation. From these typical results, the following parameters were defined to characterise the freezing process (see Fig. 5): (i) temperature of spontaneous nucleation, T_{sn}; (ii) freezing point, T_f; (iii) residual volumetric unfrozen water content, θ_r (the value recorded at temperature equal to T_{sn}); (iv) duration of the temperature plateau, t_p; and (v) duration of the freezing process, t_f.

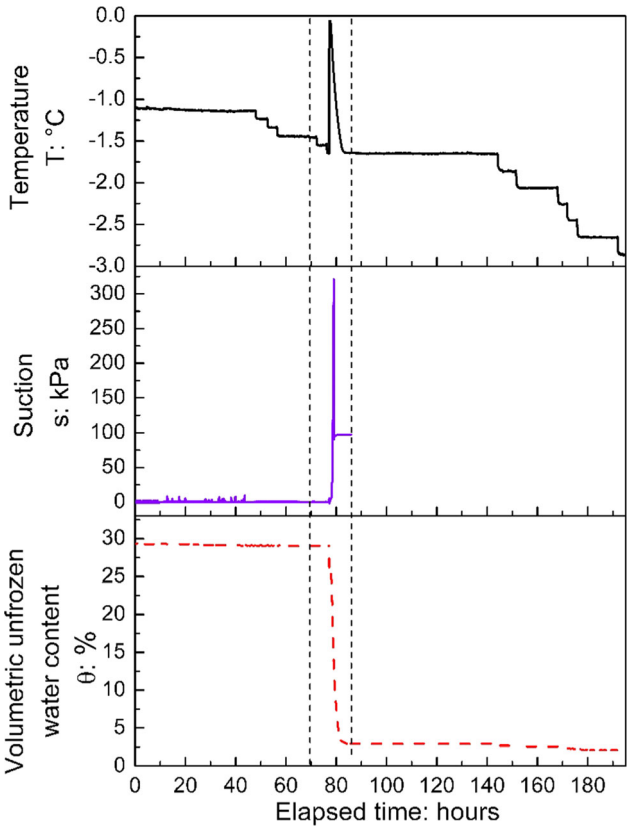

Fig. 4 Soil temperature, volumetric unfrozen water content and suction versus elapsed time during the cooling path of test S10-T1

After the freezing process (from 83 h), decrease in temperature induced slight decrease in volumetric unfrozen water content (see Fig. 4), while soil suction measurement was no longer available because of the cavitation of the tensiometer.

Figure 6 shows the results of test S10-T1 during the heating path. During this path, temperature was increased by steps of 0.2 °C from −2.8 to 0 °C. It induced thawing of frozen water (corresponding to a gradual increase in unfrozen water content).

From the results shown in Figs. 4, 5 and 6, volumetric unfrozen water content obtained at the end of each step is plotted versus the corresponding soil temperature for test S10-T1 in Fig. 7. These results correspond to the SFCC of

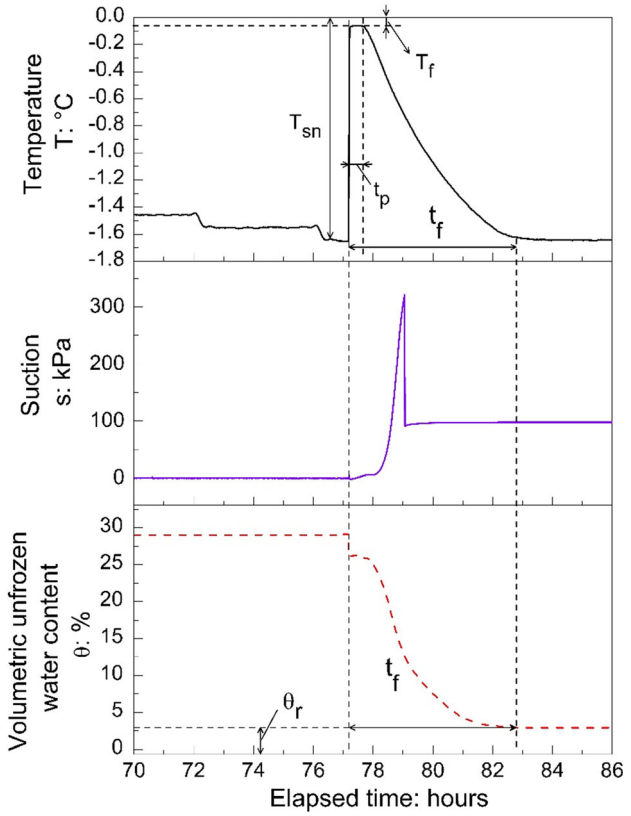

Fig. 5 Soil temperature, volumetric unfrozen water content and suction versus elapsed time during the freezing process of test S10-T1 (detailed view from 70 to 86 h)

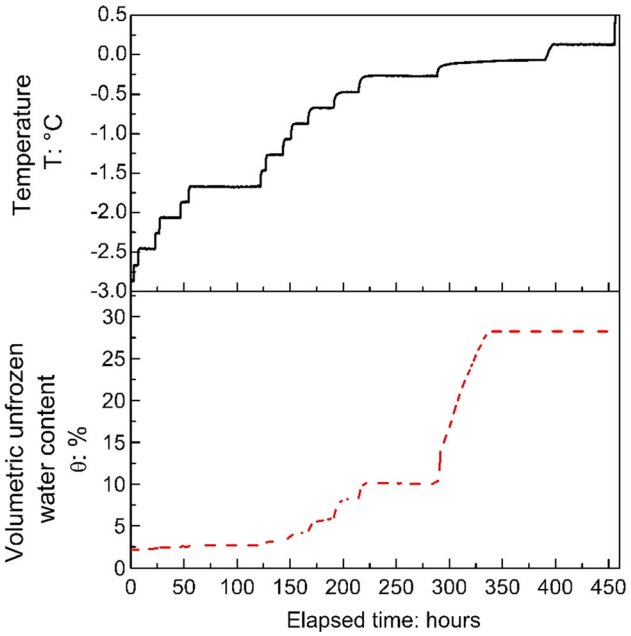

Fig. 6 Soil temperature and volumetric unfrozen water content versus elapsed time during the heating path of test S10-T1

soil S10 obtained from test S10-T1, which include both freezing and thawing paths.

3.2 Effects of fines content

SFCC of all soils is shown in Fig. 8 where volumetric unfrozen water content was plotted versus temperature. As the initial volumetric water content (which depends on soil dry density) was different from one soil to the others, it is thus difficult to analyse the effect of fines content from these results. For this reason, volumetric unfrozen water content was used to calculate unfrozen water degree of saturation ($S_r = \theta/\theta_{sat}$; where θ_{sat} is the volumetric unfrozen water content at saturate state). Figure 9 shows SFCC of all soils where unfrozen degree of saturation was plotted versus temperature. For each soil, from the initial saturated state, when soil temperature decreased from 0 °C, soil remained saturated with unfrozen water. When temperature reached the temperature of spontaneous nucleation, freezing was triggered inducing significant decrease in unfrozen water degree of saturation. After this step, cooling induced only slight decrease in unfrozen water degree of saturation. During the heating path, unfrozen water degree of saturation increased gradually with temperature and the relationship between these two quantities was significantly different from the cooling path for all soils.

In order to quantitatively assess the effects of fines content, temperatures of spontaneous nucleation T_{sn} and freezing point T_f were plotted versus fines content (Fig. 10). The results show that the temperature of freezing

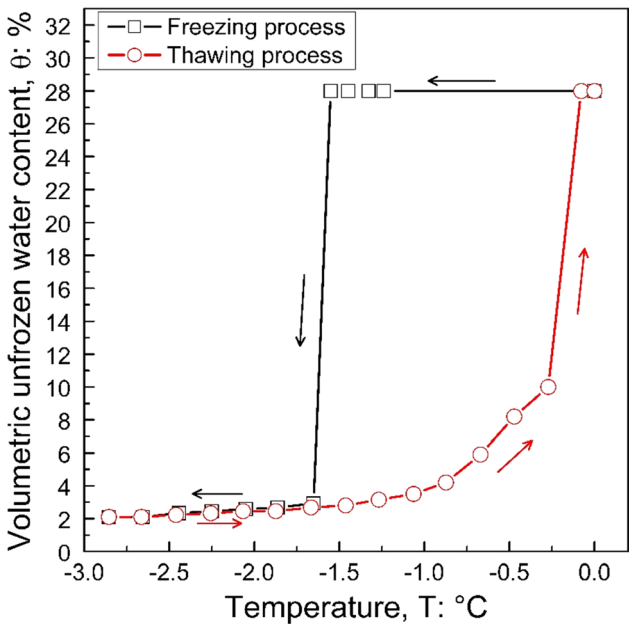

Fig. 7 Soil freezing characteristic curve determined from test S10-T1

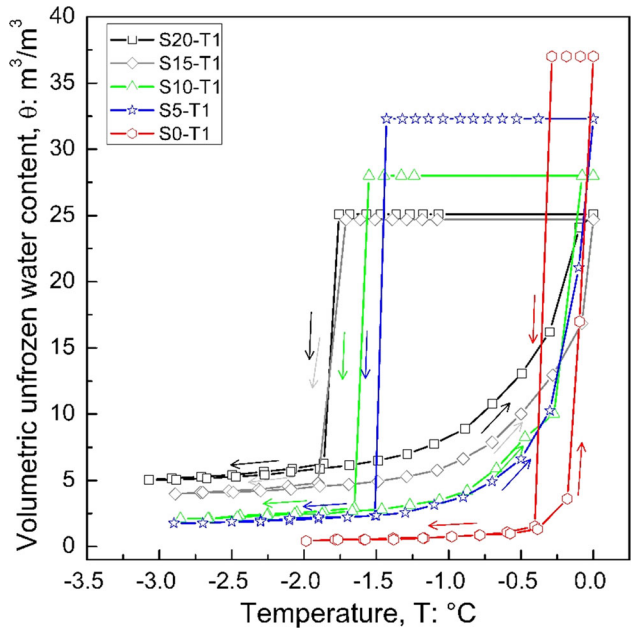

Fig. 8 Soil freezing characteristic curve (volumetric unfrozen water content versus temperature) for all soils

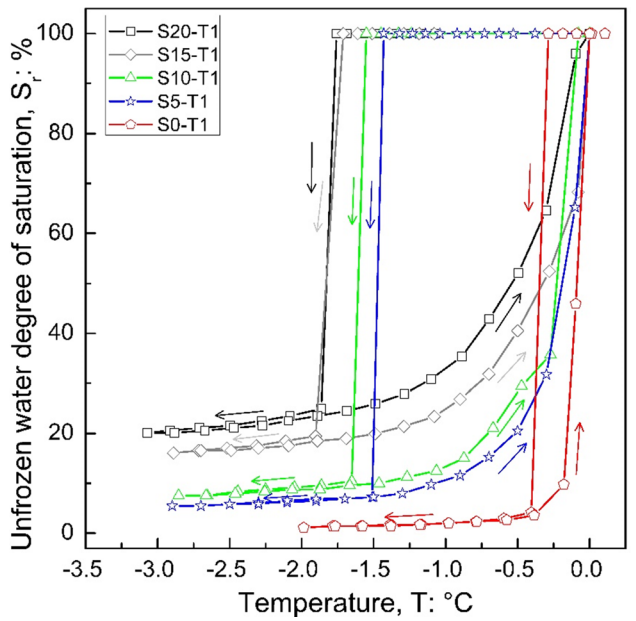

Fig. 9 Soil freezing characteristic curve (unfrozen water degree of saturation versus temperature) for all soils

point was close to 0 °C for all soils. The results were quite repeatable (with variation less than 0.1 °C) and only a slight trend of decrease of T_f when fines content increase could be observed. For T_{sn}, results showed a higher scattering (up to 0.5 °C, except for test at 0% of clay content where this value varied from −0.4 to −1.5 °C). In general, T_{sn} is lower at a higher clay content.

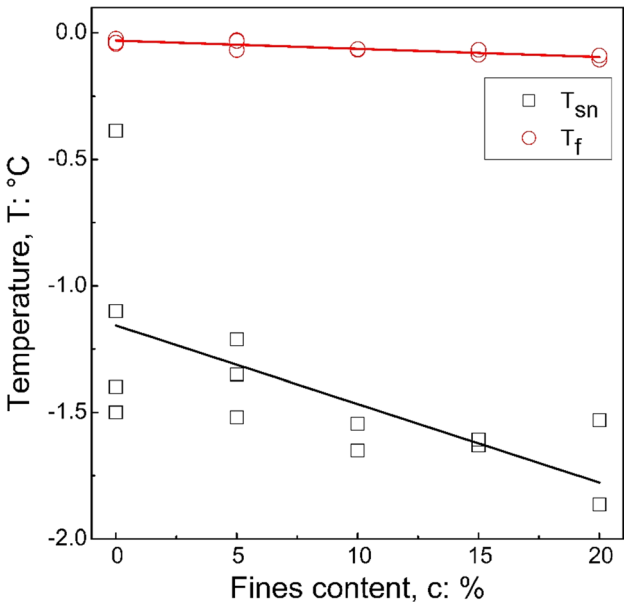

Fig. 10 Temperatures of spontaneous nucleation and freezing point versus fines content

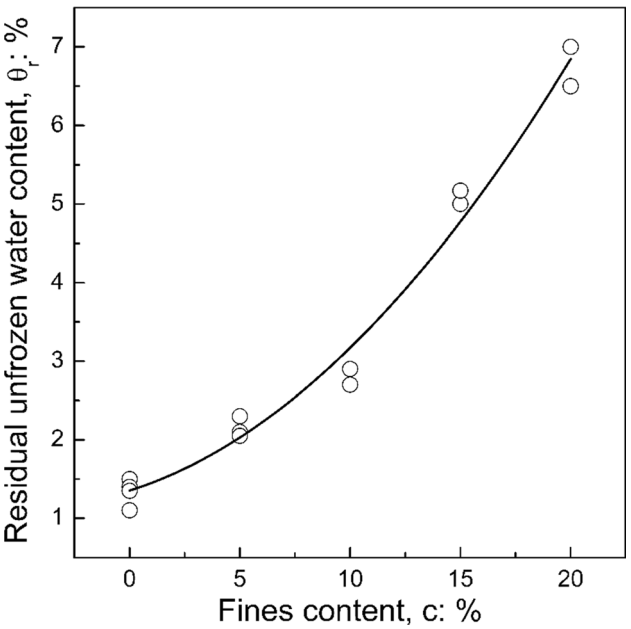

Fig. 11 Residual unfrozen water content versus fines content

Figure 11 shows the residual unfrozen water content θ_r (the value determined at a temperature equal to T_{sn}, see Fig. 5) versus fines content. A good repeatability (with a scattering of 0.5%) could be observed. The results show that residual unfrozen water content was higher at a higher fines content.

Figure 12 presents the duration of the temperature plateau t_p and the duration of the freezing process t_f (see the definition on Fig. 5) versus fines content. Results of t_p were

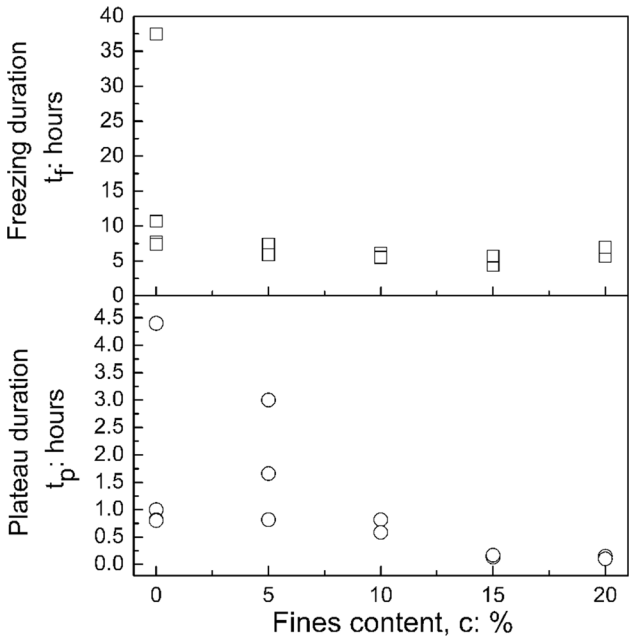

Fig. 12 Duration of the temperature plateau and duration of the freezing process versus fines content

quite scattering for 0 and 5% of fines content, varying from 0.80 to 4.40 h. They were more repeatable at higher fines contents. A general decrease of this duration when the fines contents increased could be observed. Results of t_f varied between 5 and 10 h (except one test, S0-T1 where it was very long, 37.50 h). These results did not show any clear trend.

Table 5 shows the obtained characteristic parameters of all tests for better comparison.

Table 5 Summary of characteristic parameters in freezing of tests

Test no	Fines content (%)	T_{sn} (°C)	T_f (°C)	θ_r (–)	t_p (h)	t_f (h)
S20-T1	20	−1.86	−0.11	6.5	0.15	5.65
S20-T2	20	−1.53	−0.09	7.0	0.10	6.95
S15-T1	15	−1.61	−0.07	5.2	0.17	5.70
S15-T2	15	−1.63	−0.09	5.0	0.13	4.00
S10-T1	10	−1.65	−0.07	2.9	0.58	5.50
S10-T2	10	−1.55	−0.06	2.7	0.80	6.10
S5-T1	5	−1.52	−0.03	2.3	0.82	5.90
S5-T2	5	−1.21	−0.07	2.1	3.10	7.35
S5-T3	5	−1.35	−0.03	2.1	1.70	7.40
S0-T1	0	−0.39	−0.04	1.5	4.40	37.50
S0-T2	0	−1.51	−0.02	1.10	1.00	7.70
S0-T3	0	−1.10	−0.04	1.40	0.80	10.70
S0-T4	0	−1.40	−0.02	1.35	0.80	7.40

4 Discussion

In this study, in order to determine the relationship between unfrozen water content and temperature during a freezing–thawing cycle, large soil specimens (150 mm in height and 150 mm in diameter) were prepared in order to embed several sensors within the soil mass. To minimise thermal and any other gradients, soil temperature was changed by small steps and equilibrium was checked at the end of each step prior the subsequent step. At equilibrium, the soil temperature and unfrozen water content were thus supposed to be homogeneous within the specimen. Similar large soil specimens were equally used in previous studies investigating SFCC with TDR method for measurement of unfrozen water content [54, 57, 80, 90]. Smaller specimens were used when measurements were performed by pulsed-NMR method [47, 66, 68]. In several previous works, specimens were immerged in a cooling bath with constant cooling rate or at low temperature (between −15 and −30 °C) and kept for several hours [14, 48, 74, 75]. For determining SFCC, unfrozen water content was measured at various controlled temperatures [34, 47, 54, 57, 80, 90]. The difference between two successive controlled temperatures in these studies varies between 0.3 and 5 °C. In the present work, temperature steps of 0.1 and 0.2 °C were chosen before the occurrence of freezing phenomenon and afterwards, respectively, in order to determine more accurately the freezing point, the temperature of spontaneous nucleation and the SFCC.

The measurement of unfrozen water content in the present study was converted from the measurement of apparent dielectric constant. In this study, under the influence of temperature, dielectric constant of each phase in soils changes, particularly those of water and ice [27, 79]. Several models exist to estimate moisture content from unfrozen soil apparent dielectric constant [15, 28, 51, 55, 57, 60, 63, 71, 77]. The most used is Topp's empirical model [71], but it is not compatible with frozen soils [60, 61, 93]. Otherwise, Smith and Tice [60] proposed a model based on comparison of unfrozen water content measured from NMR and TDR methods for 25 soils covering a wide range of specific surface areas. For this reason, in the present work, the model of Smith and Tice [60], which provides an accuracy of ± 3% compared to measurements from NMR method, was used for frozen soils.

Hysteresis of SFCC (difference between the freezing and the thawing curves) is usually attributed to the same factors inducing hysteresis in SWCC, such as the effect of electrolytes, pore geometry, pore blocking, effect of contact angle and change in pore structure [54]. Actually, in a freezing process, increasing solute concentration by forming ice from water increases the effect of electrolyte.

Otherwise, forming ice also changes soil skeleton that affects matric potentials of soils. In addition, the hysteric behaviour is also mainly attributed to supercooling of pore water [16, 68, 70, 90]. Instead of freezing at 0 °C, pore water is necessarily supercooled at lower temperature. In the present work, an insignificant hysteresis of θ_u was observed for all soils below T_{sn} (at frozen state). First, the effect of electrolytes can be ignored. Second, temperature below T_{sn} of −1 to −2 °C corresponds to a suction of 1 to 2.5 MPa following the Clapeyron equation. This high range of suction corresponds mainly to water in micropore (intra-aggregates) in the clay matrix where SWCC is also reversible. As a result, hysteresis of SFCC observed in the present work could be contributed mainly to supercooling. After the triggering of freezing, SFCC obtained at temperature lower than T_{sn} was generally reversible (see Figs. 8 and 9).

Results shown in Fig. 9 demonstrate significant effect of fines content on the thawing path of SFCC; at a given temperature, a higher unfrozen water degree of saturation was obtained at a higher fines content. These results are consistent with the findings of previous works [45, 68, 69, 91]. Following these studies, Gibbs–Thompson equation can be used to relate the pore-size distribution and the thawing path of SFCC; a lower temperature corresponds to a smaller pore. In the present work, soil having higher fines content would have a larger volume of micropores (inter-aggregates and intra-aggregates pores) a lower volume of macropores (space between sand particles).

T_{sn} determined in this study can be associated with supercooling. Figure 10 shows that this parameter generally decreased with an increase in fines content and it was measured with a relatively high scattering. For bulk water, T_{sn} depends on numerous factors such as sample volume, cooling velocity, the presence and concentration of solutes, the presence of solid impurities, and effects of external fields (impulse waves, electromagnetic radiation, etc.) [23, 41, 73]. In the case of soils, additional factors can be soil components and their fractions. Many studies determined T_{sn} of various soils and found that increasing clay content in soils decreases temperature of spontaneous nucleation to lower range [4, 90]. These studies focussed on clays or clay and silt, and these results agree with sandy soils in the present study. It is noted that the supercooling is considered as a necessary phase to activate nucleation process and it appears in both cases, either in free pure water or within the porous volume of soils. Because of the high value of released latent heat, about 334 J/g, which appears during nucleation process, water needs to be supercooled at T_{sn} for equilibrating energy before crystallization. According to Yershov [82], T_{sn} is remarked as the temperature at which embryo nuclei form and grow to the critical sizes, about 472 H_2O corresponding to 10^{-26} m^3. The relatively high scattering of results obtained in the present work can be thus explained by the random behaviour of the crystallization process. The slight effect of fines content on T_{sn} can be explained by the effect of soil pore-size distribution on the supercooling: soil having a higher fines content would have higher volume of micropores, and T_{sn} is generally lower in a smaller pore.

Numerous studies investigated T_f and showed that T_f depends on many factors such as salt content [11, 13, 25, 48, 75], salt types [14, 74], initial water content [4], and soil types [18, 39, 42, 45, 66, 90]. In the present study, T_f was found close to 0 °C for all soils. This result can be explained by two main reasons: soils were studied at saturated state, and fines content is sufficiently low. Bing and Ma [14] obtained similar results with saturated sandy soil containing less than 7.5% of clay. Furthermore, freezing point remains constant also above a certain value of water content for all soils [14, 41, 78]. Actually, for the soils considered in the present study, with relatively low contents of low plasticity kaolin clay, the amount of bound water should be negligible and T_f should be similar to that of bulk pure water, i.e. close to 0 °C.

Residual unfrozen content was found higher at a higher fines content (Fig. 11). It is believed that residual unfrozen relates almost directly to the amount of specific surface of soils. According to several studies [45, 66, 68, 69, 90], unfrozen water content remaining in soils at the same temperature decreased in the following order: clay, silts, sands and gravel. Following Bing and Ma [14], only free water was frozen when freezing is triggered. Unfrozen water should then correspond to bound water. According to Tian et al. [68], the amount of bound water in soils is proportional to the thickness of the electric double layer and specific surface area. In the present study, a higher fines content corresponds to a higher specific surface area and then a higher amount of bound water.

The duration of temperature plateau, t_p, would depend then on the amount of latent heat released when freezing is triggered. This amount mainly depends on $T_{sn,}$as shown in Table 5. As the results of T_{sn} show significant scattering and a general slight increase when fines content increased (Fig. 10), similar trends were observed with t_p (Fig. 12). The duration of the freezing process, t_f, which is much longer than t_p, corresponds to the thermal diffusion of latent heat released during the whole freezing process. This duration would depend thus mainly on the thermal diffusivity of the frozen soil (which at the same time evolves during freezing).

5 Conclusions

The results obtained in this study show that fines content in sandy soils significantly influenced the soil behaviour under a freezing–thawing cycle. Based on the investigation of five levels of fines content (varying from 0 to 20%), the following conclusions can be addressed:

- When the temperature decreased from 0 °C, freezing was triggered at T_{sn} inducing a sudden decrease of θ_u from the saturated state to the residual state. Afterwards, θ_u continued to decrease but with a lower rate. The subsequent heating induced an increase of θ_u (which represents a progressive melting of frozen water).
- The thawing path of SFCC was strongly dependent on the fines content; at a given temperature, a higher θ_u was observed for a higher fines content.
- T_{sn} was higher at a higher fines content and varied between −1.0 and −2.0 °C.
- T_f varied between 0 °C and −0.2 °C, only a slight decrease of T_f with an increase in fines content was observed.
- θ_r (varied from 1 to 7%) was higher at a higher fines content.
- t_p was found scattering and slightly decreased when fines content increased.
- t_f was found independent of fines content.

The findings of the present study would be helpful to predict the soil behaviour under freezing–thawing process. That would imply several applications in cold regions and also in geotechnical engineering ground improvement by artificial ground freezing.

Funding No funding was received for conducting this study.

Data availability The datasets generated during and/or analysed during the current study are available from the corresponding author on reasonable request.

Declarations

Competing interests The authors have no competing interests to declare that are relevant to the content of this article.

References

1. Akyurt M, Zaki G, Habeebullah B (2002) Freezing phenomena in ice–water systems. Energy Convers Manag 43:1773–1789. https://doi.org/10.1016/S0196-8904(01)00129-7
2. Andersland OB, Ladanyi B (1994) An introduction to frozen ground engineering. Springer, Cham
3. Andersland OB, Ladanyi B (2004) Frozen ground engineering. Wiley, New York
4. Anderson DM (1968) Undercooling, freezing point depression, and ice nucleation of soil water. Isr J Chem 6:349–355. https://doi.org/10.1002/ijch.196800044
5. Anderson DM (1967) Ice nucleation and the substrate-ice interface. Nature 216:563–566. https://doi.org/10.1038/216563a0
6. Anderson DM, Hoekstra P (1965) Migration of interlamellar water during freezing and thawing of Wyoming bentonite. Soil Sci Soc Am J 29:498–504. https://doi.org/10.2136/sssaj1965.03615995002900050010x
7. Anderson DM, Morgenstern NR (1973) Physics, chemistry, and mechanics of frozen ground: a review. In: Permafrost: North American Contribution [to The] Second International Conference; National Academies: Washington, DC, USA. p 257
8. Anderson DM, Tice AR (1973) The unfrozen interfacial phase in frozen soil water systems. In: Physical aspects of soil water and salts in ecosystems, pp 107–124
9. Anderson DM, Tice AR (1972) Predicting unfrozen water contents in frozen soils from surface area measurements. Highw Res Rec 393:12–18
10. Arenson LU, Johansen MM, Springman SM (2004) Effects of volumetric ice content and strain rate on shear strength under triaxial conditions for frozen soil samples. Permafr Periglac Process 15:261–271. https://doi.org/10.1002/ppp.498
11. Ayers AD, Campell RB (1951) Freezing point of water in a soil as related to salt and moisture contents of the soil. Soil Sci 72:201–206
12. Bai R, Lai Y, Zhang M, Yu F (2018) Theory and application of a novel soil freezing characteristic curve. Appl Therm Eng 129:1106–1114. https://doi.org/10.1016/j.applthermaleng.2017.10.121
13. Banin A, Anderson DM (1974) Effects of salt concentration changes during freezing on the unfrozen water content of porous materials. Water Resour Res 10:124–128
14. Bing H, Ma W (2011) Laboratory investigation of the freezing point of saline soil. Cold Reg Sci Technol 67:79–88. https://doi.org/10.1016/j.coldregions.2011.02.008
15. Birchak JR, Gardner CG, Hipp JE, Victor JM (1974) High dielectric constant microwave probes for sensing soil moisture. Proc IEEE 62:93–98. https://doi.org/10.1109/PROC.1974.9388
16. Bittelli M, Flury M, Campbell GS (2003) A thermodielectric analyzer to measure the freezing and moisture characteristic of porous media. Water Resour Res, p 39.
17. Boussaid K (2005) Sols intermédiaires pour la modélisation physique: application aux fondations superficielles. École Centrale de Nantes et Université de Nantes
18. Cannell GH, Gardner WH (1959) Freezing-point depressions in stabilized soil aggregates, synthetic soil, and quartz sand. Soil Sci Soc Am J 23:418–422. https://doi.org/10.2136/sssaj1959.03615995002300060018x
19. Chen SL, Lee TS (1998) A study of supercooling phenomenon and freezing probability of water inside horizontal cylinders. Int J Heat Mass Transf 41:769–783. https://doi.org/10.1016/S0017-9310(97)00134-8
20. Dall'Amico M (2010) Coupled water and heat transfer in permafrost modeling. University of Trento
21. Darrow MM (2011) Thermal modeling of roadway embankments over permafrost. Cold Reg Sci Technol 65:474–487. https://doi.org/10.1016/j.coldregions.2010.11.001
22. Enninful HRNB, Schneider D, Kohns R et al (2020) A novel approach for advanced thermoporometry characterization of mesoporous solids: transition kernels and the serially connected pore model. Microporous Mesoporous Mater 309:110534. https://doi.org/10.1016/j.micromeso.2020.110534

23. Fletcher NH (1970) The chemical physics of ice. Press Cambridge, England, p 111
24. Ge S, McKenzie J, Voss C, Wu Q (2011) Exchange of groundwater and surface-water mediated by permafrost response to seasonal and long term air temperature variation. Geophys Res Lett 38:1–6. https://doi.org/10.1029/2011GL047911
25. Han Y, Wang Q, Kong Y et al (2018) Experiments on the initial freezing point of dispersive saline soil. CATENA 171:681–690. https://doi.org/10.1016/j.catena.2018.07.046
26. Han L, Ye G, Li Y et al (2016) In situ monitoring of frost heave pressure during cross passage construction using ground-freezing method. Can Geotech J 53:530–539. https://doi.org/10.1139/cgj-2014-0486
27. Haynes WM (2016) CRC handbook of chemistry and physics, 97th edn. CRC Press, Boca Raton
28. He H, Dyck M (2013) Application of multiphase dielectric mixing models for understanding the effective dielectric permittivity of frozen soils. Vadose Zo J 12. https://doi.org/10.2136/vzj2012.0060
29. He Z, Teng J, Yang Z et al (2020) An analysis of vapour transfer in unsaturated freezing soils. Cold Reg Sci Technol 169:102914. https://doi.org/10.1016/j.coldregions.2019.102914
30. Hoekstra P (1966) Moisture movement in soils under temperature gradients with the cold-side temperature below freezing. Water Resour Res 2:241–250
31. Horiguchi K, Miller RD (1980) Experimental studies with frozen soil in an "ice sandwich" permeameter. Cold Reg Sci Technol 3:177–183. https://doi.org/10.1016/0165-232X(80)90023-3
32. Hu G, Zhao L, Zhu X et al (2020) Review of algorithms and parameterizations to determine unfrozen water content in frozen soil. Geoderma 368:114277. https://doi.org/10.1016/j.geoderma.2020.114277
33. Ishizaki T, Maruyama M, Furukawa Y, Dash J (1996) Premelting of ice in porous silica glass. J Cryst Growth 163:455–460
34. Jia H, Ding S, Wang Y et al (2019) An NMR-based investigation of pore water freezing process in sandstone. Cold Reg Sci Technol 168:102893. https://doi.org/10.1016/j.coldregions.2019.102893
35. Kebria MM, Na S, Yu F (2022) An algorithmic framework for computational estimation of soil freezing characteristic curves. Int J Numer Anal Methods Geomech 46:1544–1565. https://doi.org/10.1002/nag.3356
36. Kolaian JH, Low PF (1963) Calorimetric determination of unfrozen water in montmorillonite pastes. Soil Sci 95:376–384
37. Koopmans RWR, Miller RD (1966) Soil freezing and soil water characteristic curves. Soil Sci Soc Am J 30:680–685
38. Kozlowski T (2003) A comprehensive method of determining the soil unfrozen water curves. Cold Reg Sci Technol 36:71–79. https://doi.org/10.1016/S0165-232X(03)00007-7
39. Kozlowski T (2004) Soil freezing point as obtained on melting. Cold Reg Sci Technol 38:93–101. https://doi.org/10.1016/j.coldregions.2003.09.001
40. Kozlowski T (2007) A semi-empirical model for phase composition of water in clay–water systems. Cold Reg Sci Technol 49:226–236. https://doi.org/10.1016/j.coldregions.2007.03.013
41. Kozlowski T (2009) Some factors affecting supercooling and the equilibrium freezing point in soil–water systems. Cold Reg Sci Technol 59:25–33. https://doi.org/10.1016/j.coldregions.2009.05.009
42. Kozlowski T (2016) A simple method of obtaining the soil freezing point depression, the unfrozen water content and the pore size distribution curves from the DSC peak maximum temperature. Cold Reg Sci Technol 122:18–25. https://doi.org/10.1016/j.coldregions.2015.10.009
43. Kozlowski T, Nartowska E (2013) Unfrozen water content in representative bentonites of different origin subjected to cyclic freezing and thawing. Vadose Zo J 12. https://doi.org/10.2136/vzj2012.0057
44. Kruse AM, Darrow MM (2017) Adsorbed cation effects on unfrozen water in fine-grained frozen soil measured using pulsed nuclear magnetic resonance. Cold Reg Sci Technol 142:42–54. https://doi.org/10.1016/j.coldregions.2017.07.006
45. Li Z, Chen J, Sugimoto M (2020) Pulsed NMR measurements of unfrozen water content in partially frozen soil. J Cold Reg Eng 34:04020013. https://doi.org/10.1061/(ASCE)CR.1943-5495.0000220
46. Liu Z, Yu X (2013) Physically based equation for phase composition curve of frozen soils. Transp Res Rec J Transp Res Board 2349:93–99. https://doi.org/10.3141/2349-11
47. Ma T, Wei C, Xia X et al (2017) Soil freezing and soil water retention characteristics: connection and solute effects. J Perform Constr Facil 31:1–8. https://doi.org/10.1061/(ASCE)CF.1943-5509.0000851
48. Ming F, Chen L, Li D, Du C (2020) Investigation into freezing point depression in soil caused by NaCl solution. Water 12:2232. https://doi.org/10.3390/w12082232
49. Mishima O, Stanley HE (1998) The relationship between liquid, supercooled and glassy water. Nature 396:329–335. https://doi.org/10.1038/24540
50. Mu QY, Zhou C, Ng CWW, Zhou GGD (2019) Stress effects on soil freezing characteristic curve: equipment development and experimental results. Vadose Zo J 18:1–10. https://doi.org/10.2136/vzj2018.11.0199
51. Nagare RM, Schincariol RA, Quinton WL, Hayashi M (2011) Laboratory calibration of time domain reflectometry to determine moisture content in undisturbed peat samples. Eur J Soil Sci 62:505–515. https://doi.org/10.1111/j.1365-2389.2011.01351.x
52. Patterson DE, Smith MW (1981) The measurement of unfrozen water content by time domain reflectometry: results from laboratory tests. Can Geotech J 18:131–144. https://doi.org/10.1139/t81-012
53. Petrov O, Furó I (2006) Curvature-dependent metastability of the solid phase and the freezing-melting hysteresis in pores. Phys Rev E 73:011608. https://doi.org/10.1103/PhysRevE.73.011608
54. Ren J, Vanapalli SK (2019) Comparison of soil-freezing and soil-water characteristic curves of two Canadian soils. Vadose Zo J 18:1–14. https://doi.org/10.2136/vzj2018.10.0185
55. Roth K, Schulin R, Fluhler H, Attinger W (1990) Calibration of time domain reflectometry for water content measurement using a composite dielectric approach. WATER Resour Res 26:2267–2273
56. Russo G, Corbo A, Cavuoto F, Autuori S (2015) Artificial ground freezing to excavate a tunnel in sandy soil. Measurements and back analysis. Tunn Undergr Sp Technol 50:226–238. https://doi.org/10.1016/j.tust.2015.07.008
57. Schafer H, Beier N (2020) Estimating soil-water characteristic curve from soil-freezing characteristic curve for mine waste tailings using time domain reflectometry. Can Geotech J 57:73–84. https://doi.org/10.1139/cgj-2018-0145
58. Schreiber A, Ketelsen I, Findenegg GH (2001) Melting and freezing of water in ordered mesoporous silica materials. Phys Chem Chem Phys 3:1185–1195. https://doi.org/10.1039/b010086m
59. Sheshukov AY, Nieber JL (2011) One-dimensional freezing of nonheaving unsaturated soils: Model formulation and similarity solution. Water Resour Res 47:1–17. https://doi.org/10.1029/2011WR010512
60. Smith MW, Tice AR (1988) Measurement of the unfrozen water content of soils: comparison of NMR and TDR methods. CRREL report, pp 88–18.
61. Spaans EJ, Baker JM (1995) Examining the use of time domain reflectometry for measuring liquid water content in frozen soil.

Water Resour Res 31:2917–2925. https://doi.org/10.1029/95WR02769
62. Spaans EJA, Baker JM (1996) The soil freezing characteristic: its measurement and similarity to the soil moisture characteristic. Soil Sci Soc Am J 60:13–19
63. Stähli M, Stadler D (1997) Measurement of water and solute dynamics in freezing soil columns with time domain reflectometry. J Hydrol 195:352–369. https://doi.org/10.1016/S0022-1694(96)03227-1
64. Sun K, Zhou A (2021) A multisurface elastoplastic model for frozen soil. Acta Geotech 16:3401–3424. https://doi.org/10.1007/s11440-021-01391-7
65. Suzuki S (2004) Dependence of unfrozen water content in unsaturated frozen clay soil on initial soil moisture content. Soil Sci Plant Nutr 50:603–606. https://doi.org/10.1080/00380768.2004.10408518
66. Teng J, Kou J, Yan X et al (2020) Parameterization of soil freezing characteristic curve for unsaturated soils. Cold Reg Sci Technol 170:102928. https://doi.org/10.1016/j.coldregions.2019.102928
67. Teng J, Zhong Y, Zhang S, Sheng D (2021) A mathematic model for the soil freezing characteristic curve: the roles of adsorption and capillarity. Cold Reg Sci Technol 181:103178. https://doi.org/10.1016/j.coldregions.2020.103178
68. Tian H, Wei C, Wei H, Zhou J (2014) Freezing and thawing characteristics of frozen soils: Bound water content and hysteresis phenomenon. Cold Reg Sci Technol 103:74–81. https://doi.org/10.1016/j.coldregions.2014.03.007
69. Tice AR, Anderson DM, Banin A (1976) The prediction of unfrozen water contents in frozen soils from liquid limit determinations. Department of Defense, Army, Corps of Engineers, Cold Regions Research and Engineering Laboratory
70. Tice AR, Anderson DM, Sterrett KF (1982) Unfrozen water contents of submarine permafrost determined by nuclear magnetic resonance. In: Developments in Geotechnical Engineering. pp 135–146
71. Topp GC, Davis JL, Annan AP (1980) Electromagnetic determination of soil water content: Measurements in coaxial transmission lines. Water Resour Reserch 16:574–582
72. Torrance JK, Schellekens FJ (2006) Chemical factors in soil freezing and frost heave. Polar Rec (Gr Brit) 42:33–42. https://doi.org/10.1017/S0032247405004894
73. Uzu Y, Sano I (1965) On the freezing of the droplets of aqueous solutions. J Meteorol Soc Japan Ser II 43:290–292
74. Wan X, Lai Y, Wang C (2015) Experimental study on the freezing temperatures of saline silty soils. Permafr Periglac Process 26:175–187. https://doi.org/10.1002/ppp.1837
75. Wan X, Liu E, Qiu E (2021) Study on ice nucleation temperature and water freezing in saline soils. Permafr Periglac Process 32:119–138. https://doi.org/10.1002/ppp.2081
76. Watanabe K, Mizoguchi M (2002) Amount of unfrozen water in frozen porous media saturated with solution. Cold Reg Sci Technol 34:103–110. https://doi.org/10.1016/S0165-232X(01)00063-5
77. Watanabe K, Wake T (2009) Measurement of unfrozen water content and relative permittivity of frozen unsaturated soil using NMR and TDR. Cold Reg Sci Technol 59:34–41. https://doi.org/10.1016/j.coldregions.2009.05.011
78. Wen Z, Ma W, Feng W et al (2012) Experimental study on unfrozen water content and soil matric potential of Qinghai-Tibetan silty clay. Environ Earth Sci 66:1467–1476. https://doi.org/10.1007/s12665-011-1386-0
79. Wraith JM, Or D (1999) Temperature effects on soil bulk dielectric permittivity measured by time domain reflectometry: experimental evidence and hypothesis development. Water Resour Res 35:361–369
80. Wu M, Tan X, Huang J et al (2015) Solute and water effects on soil freezing characteristics based on laboratory experiments. Cold Reg Sci Technol 115:22–29. https://doi.org/10.1016/j.coldregions.2015.03.007
81. Ye M, Pan F, Wu Y-S et al (2007) Assessment of radionuclide transport uncertainty in the unsaturated zone of Yucca Mountain. Adv Water Resour 30:118–134. https://doi.org/10.1016/j.advwatres.2006.03.005
82. Yershov ED (2004) General geocryology. Cambridge University Press
83. Yong RN, Cheung C, Sheeran DE (1979) Prediction of salt influence on unfrozen water content in frozen soils. In: Developments in Geotechnical Engineering. pp 137–155
84. Yoshikawa K, Overduin PP (2005) Comparing unfrozen water content measurements of frozen soil using recently developed commercial sensors. Cold Reg Sci Technol 42:250–256. https://doi.org/10.1016/j.coldregions.2005.03.001
85. Yu F, Guo P, Na S (2022) A framework for constructing elastoplastic constitutive models for frozen and unfrozen soils. Int J Numer Anal Methods Geomech 46:436–466. https://doi.org/10.1002/nag.3306
86. Yu W, Zhang T, Lu Y et al (2020) Engineering risk analysis in cold regions: State of the art and perspectives. Cold Reg Sci Technol 171:102963. https://doi.org/10.1016/j.coldregions.2019.102963
87. Zhang S, Sheng D, Zhao G et al (2016) Analysis of frost heave mechanisms in a high-speed railway embankment. Can Geotech J 53:520–529. https://doi.org/10.1139/cgj-2014-0456
88. Zhang X, Sun SF, Xue Y (2007) Development and testing of a frozen soil parameterization for cold region studies. J Hydrometeorol 8:690–701. https://doi.org/10.1175/JHM605.1
89. Zhang S, Teng J, He Z et al (2016) Canopy effect caused by vapour transfer in covered freezing soils. Géotechnique 66:927–940. https://doi.org/10.1680/jgeot.16.P.016
90. Zhang M, Zhang X, Lai Y et al (2020) Variations of the temperatures and volumetric unfrozen water contents of fine-grained soils during a freezing–thawing process. Acta Geotech 15:595–601. https://doi.org/10.1007/s11440-018-0720-z
91. Zhang H, Zhang J, Zhang Z et al (2020) Variation behavior of pore-water pressure in warm frozen soil under load and its relation to deformation. Acta Geotech 15:603–614. https://doi.org/10.1007/s11440-018-0736-4
92. Zhou J, Wei C, Lai Y et al (2018) Application of the generalized clapeyron equation to freezing point depression and unfrozen water content. Water Resour Res 54:9412–9431. https://doi.org/10.1029/2018WR023221
93. Zhou X, Zhou J, Kinzelbach W, Stauffer F (2014) Simultaneous measurement of unfrozen water content and ice content in frozen soil using gamma ray attenuation and TDR. Water Resour Res 50:9630–9655. https://doi.org/10.1002/2014WR015640
94. Zhou X, Zhou J, Kinzelbach W, Stauffer F (2014) Simultaneous measurement of unfrozen water content and ice content in frozen soil using gamma ray attenuation and TDR. J Am Water Resour Assoc 5:2–2. https://doi.org/10.1111/j.1752-1688.1969.tb04897.x
95. Zhou Y, Zhou J, Shi X, Zhou G (2019) Practical models describing hysteresis behavior of unfrozen water in frozen soil

based on similarity analysis. Cold Reg Sci Technol 157:215–223. https://doi.org/10.1016/j.coldregions.2018.11.002